



TITLE:

Magnetic susceptibility of the one-dimensional polymeric phase of RbC60

AUTHOR(S):

Saito, T; Akita, Y; Tanaka, K

CITATION:

Saito, T ...[et al]. Magnetic susceptibility of the one-dimensional polymeric phase of RbC60. PHYSICAL REVIEW B 2000, 61(23): 16091-16096

ISSUE DATE:

2000-06-15

URL:

<http://hdl.handle.net/2433/39842>

RIGHT:

Copyright 2000 American Physical Society

Magnetic susceptibility of the one-dimensional polymeric phase of RbC_{60}

Takeshi Saito, Yosuke Akita, and Kazuyoshi Tanaka*

Department of Molecular Engineering, Graduate School of Engineering, Kyoto University, Sakyo-ku, Kyoto 606-8501, Japan

(Received 14 December 1999)

Detailed magnetic susceptibility measurements of the RbC_{60} polymeric phase have been carried out. A decrease in the susceptibility on cooling below 50 K consistent with the temperature dependence of the electron spin resonance intensity hitherto reported has been observed. It has been shown that this temperature dependence can be interpreted in terms of the spin density wave scenario in a consistent manner and that the density of states at the Fermi level can be estimated as 11.9 states/(eV C_{60}^{-}). This value is in reasonable agreement with 8 states/(eV C_{60}^{-}) estimated by the tight-binding band structure calculation.

I. INTRODUCTION

Several kinds of alkali-metal-doped polymeric C_{60} materials connected by covalent bonds without any additional linking groups have recently been considerably paid attention to.¹⁻³ In particular, AC_{60} ($A = \text{K}, \text{Rb}, \text{and Cs}$), first reported as the electrically conducting alkali fulleride linear-chain polymer,⁴ is currently of high interest. Stephens *et al.* have first reported a relatively simple crystal structure of polymeric AC_{60} with parallel polymer chains consisting of covalently bonded C_{60} molecules.¹ Recently, Launois *et al.*⁵ have found that the single crystal of the polymeric phase of RbC_{60} is actually monoclinic, space group $I_{2/m}$ (without measurement of the monoclinic angle). Bendele *et al.*⁶ have reached a similar conclusion with the monoclinic angle $\beta = 90.3^\circ$.

One of the most interesting aspects of these materials is their low-dimensional-like electronic properties, which are different among the AC_{60} polymers with each kind of A . In the electron spin resonance (ESR) study, it was suggested that the polymeric RbC_{60} and CsC_{60} are quasi-one-dimensional (1D) conductors and that the phase transition at 50 K causes antiferromagnetic (AF) ordering of spin density waves⁴ (SDW) under that temperature, while the KC_{60} polymeric phase remains almost an isotropic metal.⁷ Such a 3D metallic property of KC_{60} has been confirmed by nuclear magnetic resonance (NMR).⁸ On the other hand, the nature of the ground state of RbC_{60} and CsC_{60} is still under debate. Recently, Jánossy *et al.* have observed the AF magnetic resonance⁹ (AFMR) in powder samples of RbC_{60} and CsC_{60} at high frequencies (75, 150, and 225 GHz) and their experimental data supported the above scenario of the quasi-1D SDW system. Bennati *et al.*¹⁰ have reached similar conclusions from a high-field ESR investigation. However, they have added that all the features in the ESR results interpreted by AFMR scenario can also be well explained within the spin-glass model. Moreover, in polymeric CsC_{60} , it has been reported that detailed ^{13}C - and ^{133}Cs -NMR investigations revealed the coexistence of a spin-Peierls (non-magnetic) state with 3D magnetic order below 13.8 K.¹¹

Meanwhile, a theoretical study on the RbC_{60} polymeric phase¹² has led to different predictions from the experimental results concerning the dimensionality of the corresponding

phase; the crystal orbital (CO) study on this compound on the basis of the tight-binding calculation including both σ and π electrons instead favors a dimensionality of three. Therefore, both the dimensionality of the electronic structure and nature of the low-temperature phase currently seem to remain open questions.

In general the ESR data do not correspond to the static magnetic susceptibility and, moreover, the former hardly allows us to discuss the magnetic behavior around the transition temperature of the magnetically ordered state in a quantitative manner.⁷ In the present article, we present the measurement results of bulk magnetization of the polymeric phase of RbC_{60} by a superconducting quantum interference device (SQUID) magnetometer and discussion of the above-mentioned problem by means of quantitative analysis of the data of temperature dependence of the static magnetic susceptibility.

II. SAMPLE PREPARATION AND CHECK

The sample was prepared by solid-phase reaction of C_{60} and Rb, the latter of which was directly generated by thermal decomposition from RbN_3 under continuous heating at 400°C for 4 days in vacuum. In order to estimate the composition of the reaction product, the x-ray photoelectron spectroscopy (XPS) measurement was performed using Mg $K\alpha$ radiation (ULVAC PHI Model 5500). The C $1s$ peak was observed at 285.4 eV and that Rb $3d_{3/2}$ and $3d_{5/2}$ peaks were observed at 110.9 and 112.3 eV, respectively. Since the N $1s$ peak was not observed at all, one could expect that RbN_3 had completely decomposed to Rb metal and N_2 during the reaction. The composition was estimated to be $\text{Rb}_{1.1}(\text{C}_{60})_{1.0}$ by the usual XPS procedure.

The structure of the RbC_{60} powder sample thus prepared was examined by the x-ray diffraction (XRD) pattern recorded at a beam line X3B1 of the National Synchrotron Light Source at Brookhaven National Laboratory with a wavelength of 1.149 02 Å. Formation of the polymeric phase was confirmed since the diffraction pattern was completely in accordance with our previous data of liquid-phase prepared RbC_{60} with lattice parameters of approximately $a = 9.1$, $b = 10.1$, and $c = 14.2$ Å.¹³

Prior to the static magnetic susceptibility measurement, the ESR data of the present sample was checked using JEOL

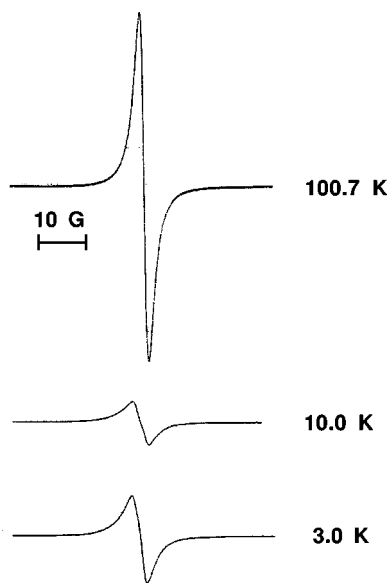


FIG. 1. ESR line shapes at selected temperatures.

JES TE-200 ESR spectrometer operated at the X band (9.4 GHz) with 100 kHz field modulation equipped with an Oxford liquid-He-flow cryostat covering the region from room temperature to 1.7 K. During a scanning for the ESR measurement at each fixed temperature, the deviation of the temperature was controlled within ± 0.2 K. The ESR signals for selected temperatures are shown in Fig. 1. In the range 50–200 K, the intensity of the ESR signal was almost temperature independent, while the peak-to-peak linewidth (ΔH_{pp}) became gradually smaller due to a decrease in temperature. Such Pauli paramagnetic behavior of the intensity and the motional narrowing of the ESR peak clearly indicate that the present sample is metallic above ~ 50 K. At 50 K, the onset of rapid broadening of the peak and the decrease of its intensity was observed and this quantity once became approximately zero around 15 K and then increased on cooling below 10 K, probably following the Curie law. These behaviors completely agree with what have been found in the aforementioned studies,^{4,7} and hence we are now in position for a further check of the static magnetic susceptibility of the RbC_{60} sample.

III. MAGNETIC SUSCEPTIBILITY MEASUREMENT

The magnetic susceptibility measurement was performed using a SQUID magnetometer (Quantum Design MPMS-5S) with the maximum magnetic field of 40 kG operating from 100.0 K to 4.5 K. The deviation of the temperature was controlled within $\pm 0.5\%$ of each fixed temperature. The core diamagnetic contribution was estimated to be 2.74×10^{-4} emu/mol from the published Pascal constants of the rubidium ion,¹⁴ and the diamagnetic susceptibility of neutral C_{60} (Ref. 15) and was corrected for all the data.

In Fig. 2 is shown the magnetic field dependence of the magnetization per mol (M_{mol}) for the RbC_{60} sample at selected temperatures. The spin-flop transition suggested by the ESR study^{9,10} could not be observed in the magnetic-field range $H=0$ –40 kG. However, it is well known that anomaly or change in the gradient of the M_{mol} - H curve characteristic of the spin-flop transition is extremely slight in

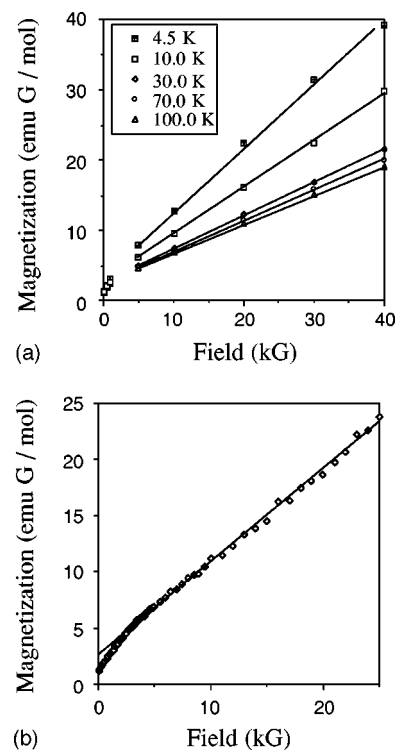


FIG. 2. (a) External magnetic field dependences of the magnetization at selected temperatures. (b) Detailed field dependence of magnetization at $T=4.5$ K.

powder sample compared with crystal.¹⁶ The existence of a very small amount of the ferromagnetic impurity is seen in Fig. 2(b), the value of which (M_s) was estimated as 2.8 emu G/mol ($\approx 3 \times 10^{20} \mu_B$ /mol, μ_B denoting the Bohr magneton). The ferromagnetic component obtained from usual Honda-Owen plot turned out to be almost temperature independent and was subtracted from all the data of the magnetic susceptibilities throughout the present article.

The temperature dependence of the static susceptibility χ_{exp} thus obtained under selected magnetic fields is shown in Fig. 3. In this magnetic field range, the shapes of the susceptibility curves are almost the same although the subtle decrease of the susceptibility is seen for 40 kG, which would

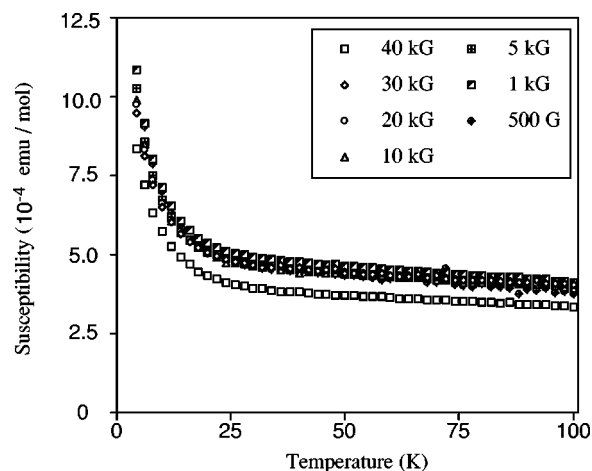


FIG. 3. Temperature dependences of the susceptibility measured under selected external field ($H=500$ G–40 kG).

be probably due to saturation of some magnetization component. It is striking that rapid decrease in χ_{exp} under 50 K was not apparently observed, being different from the ESR data mentioned above. One of the possibilities to comprehend this discrepancy would invoke the Curie-type impurity concealing behavior of the susceptibility from conduction electrons. In order to quantitatively evaluate that susceptibility, the following strategy was employed. First, χ_{exp} was decomposed into three kinds of terms as

$$\chi_{exp} = \chi_{TD} + \chi_{Curie} + \chi_{TI}, \quad (1)$$

where χ_{TD} and χ_{TI} stand for the temperature-dependent term free from the Curie contribution and the temperature-independent one, respectively, and

$$\chi_{Curie} = \frac{N_{mol} g^2 \mu_B^2 S(S+1)}{3k_B(T-\theta)}. \quad (2)$$

In Eq. (2), N_{mol} , g , S , k_B , and θ are spin concentration per mole, Landé g factor, spin quantum number, Boltzmann constant, and Weiss constant, respectively, as usual. Second, we assume that χ_{TD} becomes approximately equal to zero below 14 K and, therefore, only χ_{Curie} contributes to the temperature dependence of the susceptibility there. It is well known that the intensity of the X band ESR resonance of this compound becomes approximately equal to zero below ~ 20 K,¹⁷ and we have also obtained a similar ESR result as described above. Besides, as we mentioned in the Introduction, Jánossy *et al.* have recently reported the result of high-field ESR investigation where spin-flop-like behavior appeared at 20–15 K.⁹ Hence, we have inferred that we could safely choose to set χ_{TD} to zero below 14 K, which is sufficiently low. In Eq. (1), χ_{TI} originates from Pauli paramagnetic term, and χ_{TD} can be considered as the temperature-dependent part of the magnetic susceptibility intrinsic in the RbC_{60} polymeric phase.

In Fig. 4 is shown the fitting result of Eq. (1) to the data of $H=1$ kG. The difference of the experimental data χ_{exp} and $\chi_{Curie} + \chi_{TI}$ in Fig. 4(a) thus signifies the net of χ_{TD} , which is replotted in Fig. 4(b). This temperature dependence of χ_{TD} is consistent with that of the ESR intensity mentioned above, i.e., the ESR intensity rapidly decreases below ~ 50 K.^{4,7} A similar temperature dependence was confirmed for all the data measured under other magnetic fields.

IV. DISCUSSION

In the case for which (i) the electronic system of RbC_{60} polymeric phase is quasi-1D, and (ii) the SDW scenario defines the ground state of this substance, the susceptibility tensor of the system ought to be characterized by the two principal values, χ_{\parallel} and χ_{\perp} , χ_{\parallel} being the value for the direction parallel to the axis of easy magnetization and χ_{\perp} for the directions perpendicular to that. With these principal values, the susceptibility for the powder RbC_{60} can be expressed by

$$\frac{3}{2}\chi \left(\approx \frac{3}{2}(\chi_{exp} - \chi_{Curie}) \right) = \frac{\chi_{\parallel} + 2\chi_{\perp}}{3}. \quad (3)$$

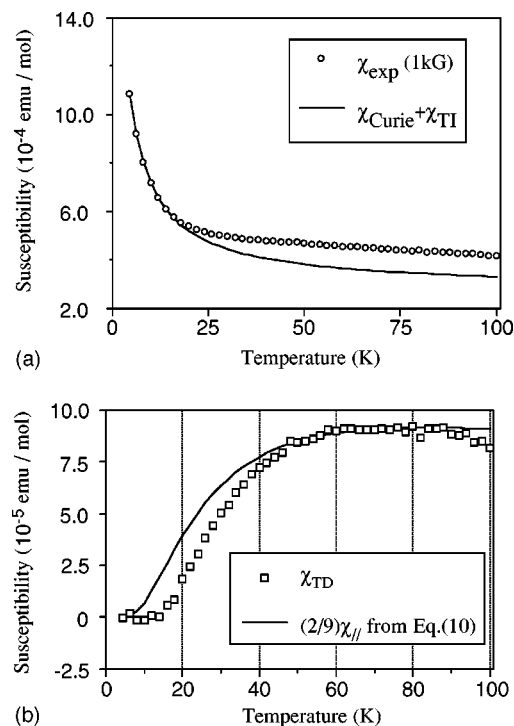


FIG. 4. (a) Temperature dependence of the susceptibility at $H = 1$ kG. The solid curve represents $\chi_{Curie} + \chi_{TI}$ (see text). (b) Temperature dependence of χ_{TD} (see text). The solid curve is the calculated $(2/9)\chi_{\parallel}$ with Eq. (10) using $\Delta/k_B = 82.3$ K.

The coefficient $(3/2)$ ahead of χ was added in consideration of the Landau diamagnetic contribution.¹⁸ Here, χ_{\perp} is expected to be almost temperature independent, similar to that in the usual antiferromagnetic system.^{16,19} According to Ref. 19, χ_{\perp} is expressed with the Pauli paramagnetic susceptibility χ_{Pauli} or the Fermi density of states (DOS) $N(\varepsilon_F)$ in the 1D metallic state as given by

$$\chi_{\perp} = \chi_{Pauli} = \mu_B^2 N(\varepsilon_F). \quad (4)$$

From Eqs. (3) and (4), $(2/3)\chi_{\perp}$ mostly corresponds to χ_{TI} .

On the other hand, χ_{\parallel} asymptotically approaches zero at $T=0$,¹⁹ and $(1/3)\chi_{\parallel}$ should correspond to χ_{TD} . χ_{\parallel} could be derived from the energy dispersion relations as follows: The conventional linear dispersion relationship appropriate for the metallic state described by

$$\varepsilon_k - \varepsilon_F = \hbar v_F (k - k_F), \quad (5)$$

where k_F and v_F correspond to the Fermi wave vector and Fermi velocity, respectively [see Fig. 5(a)]. When an energy gap is generated around the Fermi level in the SDW state, the dispersion relation should instead be given by

$$E_k - \varepsilon_F = \text{sgn}(k - k_F) \left\{ \hbar^2 v_F^2 (k - k_F)^2 + \left(\frac{\Delta}{2} \right)^2 \right\}^{1/2}, \quad (6)$$

where Δ corresponds to the energy gap as illustrated in Fig. 5(b). The Fermi DOS is obtained from the condition

$$N_{SDW}(E, \Delta) dE = N(\varepsilon_F) d\varepsilon, \quad (7)$$

where $N_{SDW}(E, \Delta)$ is the DOS in the SDW state. With Eqs. (5)–(7) one obtains,

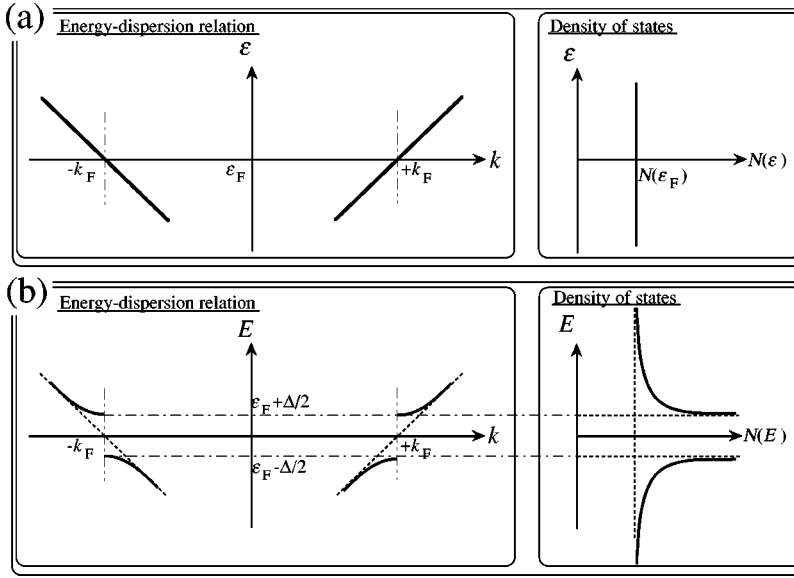


FIG. 5. The energy-dispersion relation and the energy dependence of the DOS near the Fermi wave vectors $\pm k_F$ (a) in the metallic and (b) in the SDW states.

$$\frac{N_{SDW}(E, \Delta)}{N(\varepsilon_F)} = \begin{cases} 0 & (|E| < \frac{\Delta}{2}) \\ \frac{|E|}{\{E^2 - (\Delta/2)^2\}^{1/2}} & (|E| > \frac{\Delta}{2}) \end{cases} \quad (8)$$

Thus χ_{\parallel} becomes $\mu_B^2 \langle N_{SDW}(\Delta) \rangle_T$, where $\langle N_{SDW}(\Delta) \rangle_T$ is the thermal average of $N_{SDW}(E, \Delta)$ at temperature T ,^{20,21} and hence

$$\begin{aligned} \frac{\chi_{\parallel}}{\chi_{Pauli}} &= \int_{-\infty}^{\infty} \frac{|E|}{\{E^2 - (\Delta/2)^2\}^{1/2}} \left(-\frac{\partial f}{\partial E} \right) dE \\ &= 2 \int_{\Delta/2}^{\infty} \frac{|E|}{\{E^2 - (\Delta/2)^2\}^{1/2}} \left(-\frac{\partial f}{\partial E} \right) dE, \end{aligned} \quad (9)$$

where f is the Fermi-Dirac distribution function. For $\Delta/(2k_B T) > 1/2$, Eq. (9) becomes

$$\chi_{\parallel} \approx \mu_B^2 N(\varepsilon_F) \sqrt{\frac{\pi \Delta}{k_B T}} \exp\left(-\frac{\Delta}{2k_B T}\right). \quad (10)$$

A fit of the Eq. (10) to the data above 45 K is shown as the solid curve in Fig. 4(b), affording $N(\varepsilon_F) = 11.9$ states/(eV C_{60}^-) and $\Delta/k_B = 82.3$ K. Incidentally, it should be mentioned that the DOS of the normal state of the well-known superconductor K_3C_{60} has been estimated from the static susceptibility to be 31 ± 6 states/(eV C_{60}^{3-}),²² which is about three times as much as the present result for RbC_{60} .

As shown in Fig. 4(b), χ_{TD} becomes smaller compared with the fitting curve as the temperature decreases, and this problem could be solved by introducing temperature-dependent value of energy gap $\Delta(T)$ into Eq. (10).²¹ Based on the χ_{TD} data for the temperature range $T = 20$ –60 K and Eq. (10), $\Delta(T)/k_B$ was plotted in Fig. 6. This increase of $\Delta(T)$ on cooling could correspond to the gradual opening of the pseudo-energy-gap.

In general, the behavior of electronic properties near the SDW transition temperature can be discussed using the Landau theory of phase transitions. From Ref. 19, the temperature-dependent order parameter $|\Delta|$ corresponding to

the energy gap can be obtained to be $|\Delta| = 0$ above the transition temperature, while for $T < T_{SDW}$,

$$|\Delta(T)| = \left(\frac{a_1}{2b}\right)^{1/2} (T_{SDW} - T)^{1/2}, \quad (11)$$

where a_1 and b are constant parameters and T_{SDW} the mean-field SDW transition temperature. From Eq. (11), the calculated $|\Delta(T)|/k_B$ for $T_{SDW} = 48$ K, $(a_1/2b)^{1/2} = 23.0 k_B$ is shown by the solid curve in Fig. 6, and the value of $\Delta(0)/k_B$ could be estimated from the intercept to be $\Delta(0)/k_B \approx 160$ K.

Another expression of the relation between $\Delta(0)$ and T_{SDW} is given by

$$\Delta(0) = 3.52 k_B T_{SDW}, \quad (12)$$

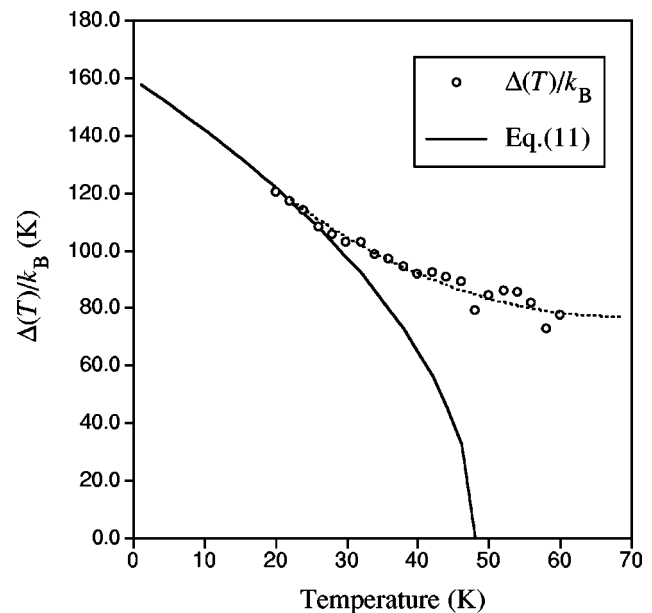


FIG. 6. Temperature dependence of $\Delta(T)/k_B$ derived from the data of χ_{TD} at $T = 20$ –60 K and Eq. (10). The solid curve represents the calculated $|\Delta(T)|/k_B$ for $T_{SDW} = 48$ K, $(a_1/2b)^{1/2} = 23.0 k_B$ from Eq. (11) (see text).

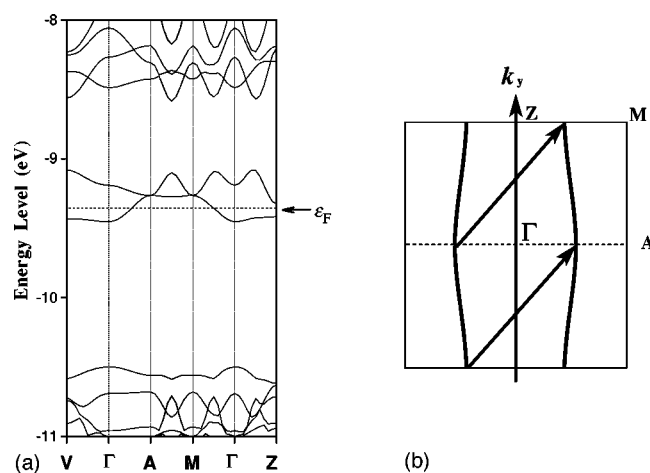


FIG. 7. (a) Band structure of RbC_{60} polymeric phase based on the tight-binding crystal orbital calculation and (b) the cross section of the Fermi surface (Ref. 23).

which has the same form as that of the well-known Bardeen-Cooper-Schrieffer (BCS) relationship between the zero-temperature gap and the transition temperature.¹⁹ With Eq. (12) and the value of $\Delta(0)/k_B \approx 160$ K, the mean-field SDW transition temperature could be derived to be $T_{SDW} \approx 45.5$ K, which seems to be approximately self-consistent.

The above-discussed SDW scenario is realized on the indispensable assumption that the electronic system of RbC_{60} polymeric phase is quasi-1D. However, the theoretical investigations on this compound has, so far, led to conflicting predictions so that the electronic and magnetic properties of this compound remain strongly 3D-like. Recently, we have carried out the investigation about change in electronic structure of RbC_{60} polymeric phase crystal ($A_{2/m}$) with various chain orientations based on the tight-binding CO calculation including both σ and π electrons.²³ It was found that the band structure of this compound is of quasi-1D for a certain limited range of chain-orientation angle, i.e., in the range $\mu = 0^\circ - 5^\circ$, where μ is the chain-orientational angle defined in Ref. 4, and there appears sufficient nesting property of the Fermi surface as shown in Fig. 7. The Fermi DOS has been estimated to be 8 states/(eV C_{60}^{-}) from this band calculation as shown in Fig. 8 to be compared with the present experimental value of DOS 11.9 states/(eV C_{60}^{-}). Note that further introduction of the relatively weak on-ball Coulomb repul-

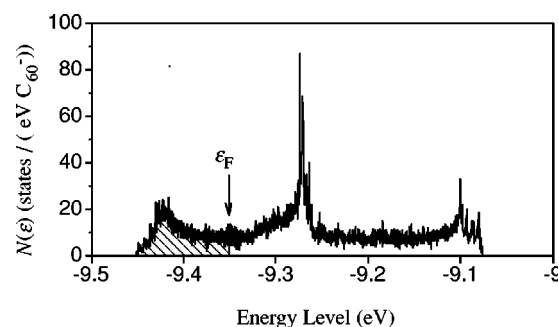


FIG. 8. The DOS diagram near the Fermi level.

sion U into the above tight-binding calculation would generally increase susceptibility proportional to the Fermi DOS.²⁴

V. CONCLUSION

We have performed a static magnetic susceptibility measurement for the RbC_{60} polymeric phase. The spin-flop transition suggested by the previous ESR study was unobserved, probably associated with the well-known fact that the anomaly in the M - H curve characteristic for the spin-flop transition is extremely slight in powder sample compared with that in crystal sample. Subtraction of the Curie paramagnetic term from the raw data gave a decrease in the susceptibility on cooling below 50 K, consistent with the temperature dependence of the ESR intensity. It was further discussed that this temperature dependence of the static susceptibility can be interpreted in terms of the SDW scenario self-consistently. The estimated Fermi DOS in metallic state is $N(\varepsilon_F) = 11.9$ states/(eV C_{60}^{-}), being about one-third of that in K_3C_{60} . The development of a more complete crystal of RbC_{60} will be of obvious importance along with further experimental investigations such as introducing partial profile relaxation and maximum-entropy methods into the XRD analysis.

ACKNOWLEDGMENTS

This work was part of the project of the Institute for Fundamental Chemistry, supported by the Japan Society for the Promotion of Science-Research for the Future Program (JSPS-RFTF96P00206). We are grateful for the aid of Professor P. W. Stephens at State University of New York at Stony Brook, with respect to the XRD measurements.

*Corresponding author.

¹P.W. Stephens, G. Bortel, G. Faigel, M. Tegze, A. Jánossy, S. Pekker, G. Oszlányi, and L. Forró, *Nature (London)* **370**, 636 (1994).

²G. Oszlányi, G. Baumgartner, G. Faigel, and L. Forró, *Phys. Rev. Lett.* **78**, 4438 (1997).

³G.M. Bendele, P.W. Stephens, K. Prassides, K. Vavekis, K. Kordatos, and K. Tanigaki, *Phys. Rev. Lett.* **80**, 736 (1998).

⁴O. Chauvet, G. Oszlányi, L. Forró, P.W. Stephens, M. Tegze, G. Faigel, and A. Jánossy, *Phys. Rev. Lett.* **72**, 2721 (1994).

⁵P. Launois, R. Moret, J. Hone, and A. Zettl, *Phys. Rev. Lett.* **81**, 4420 (1998).

⁶P.W. Stephens (private communication) (see also Ref. 13).

⁷F. Bommeli, L. Degiorgi, P. Wachter, X. Legeza, A. Jánossy, G.

Oszlányi, O. Chauvet, and L. Forró, *Phys. Rev. B* **51**, 14 794 (1995).

⁸V. Brouet, H. Alloul, Y. Yoshinari, and L. Forró, *Phys. Rev. Lett.* **76**, 3638 (1996).

⁹A. Jánossy, N. Nemes, T. Fehér, G. Oszlányi, G. Baumgartner, and L. Forró, *Phys. Rev. Lett.* **79**, 2718 (1997).

¹⁰M. Bennati, R.G. Griffin, S. Knorr, A. Grupp, and M. Mehring, *Phys. Rev. B* **58**, 15 603 (1998).

¹¹B. Simović, D. Jérôme, F. Rachdi, G. Baumgartner, and L. Forró, *Phys. Rev. Lett.* **82**, 2298 (1998).

¹²K. Tanaka, Y. Matsuura, Y. Oshima, T. Yamabe, H. Kobayashi, and Y. Asai, *Chem. Phys. Lett.* **241**, 149 (1995).

¹³T. Saito, Y. Akita, M. Tokumoto, P.W. Stephens, and K. Tanaka, *Solid State Commun.* **111**, 131 (1999).

- ¹⁴R.R. Gupta, *Numerical Data and Functional Relationships in Science and Technology New Series, Diamagnetic Susceptibility*, Landolt-Börnstein, New Series, Group III, Vol. 16 (Springer-Verlag, New York, 1986).
- ¹⁵A.P. Ramirez, R.C. Haddon, O. Zhou, R.M. Fleming, J. Zhang, S.M. McClure, and R.E. Smalley, *Science* **265**, 84 (1994).
- ¹⁶See, e.g., S. Foner, in *Magnetism*, edited by G. T. Rado and H. Suhl (Academic Press, New York, 1963), Vol. I, Chap. 9.
- ¹⁷See, e.g., K. Mizoguchi, A. Sasano, H. Sakamoto, M. Kosaka, K. Tanigaki, T. Tanaka, and T. Atake, *Synth. Met.* **103**, 2395 (1999).
- ¹⁸C. Kittel, *Introduction to Solid State Physics*, 6th ed. (Wiley, Sons, New York, 1986), Chap. 14.
- ¹⁹G. Grüner, *Density Waves in Solids* (Addison-Wesley Longman, Reading, MA, 1994), Chap. 4.
- ²⁰P.A. Lee, T.M. Rice, and P.W. Anderson, *Phys. Rev. Lett.* **31**, 462 (1973).
- ²¹D.C. Johnston, *Phys. Rev. Lett.* **52**, 2049 (1984).
- ²²W.H. Wong, M.E. Hanson, W.G. Clark, G. Grüner, J.D. Thompson, R.L. Whetten, S.-M. Huang, R.B. Kaner, F. Diederich, P. Petit, J.-J. André, and K. Holczer, *Europhys. Lett.* **18**, 79 (1992).
- ²³T. Saito, Y. Akita, H. Kobayashi, and K. Tanaka, *Synth. Metals* **113**, 45 (2000).
- ²⁴P. Fulde, *Electron Correlations in Molecules and Solids* (Springer-Verlag, New York, 1993), Chap. 10.